

BOILING-CONDENSATION HEAT TRANSFER AND FLOW CHARACTERISTICS IN ULTRATHIN LIMITED ENCLOSED SPACE BASED ON NUMERICAL SIMULATION AND VISUALIZATION EXPERIMENT

by

Li CONG^{a,b*}, Huang YING^c, and Tan JIANPING^d

^a School of Mechatronics Engineering, Jiangxi University of Science and Technology, Ganzhou, Jiangxi, China

^b Jiangxi Province Engineering Research Center for Mechanical and Electrical of Mining and Metallurgy, Ganzhou, Jiangxi, China

^c Jiangxi College of Applied Technology, Ganzhou, Jiangxi, China

^d Central South University, Changsha, Hunan, China

Original scientific paper

<https://doi.org/10.2298/TSCI210622348C>

Boiling-condensation heat transfer in ultrathin flat heat pipes are complicated and difficult to observe. In this study, a visualization experiment and simulation analysis in an ultrathin limited enclosed space were carried out. Width of the ultrathin enclosed space was 1 mm, with anhydrous ethanol as the working medium. The enclosed space was oriented vertically with the heating section on the bottom and the cooling section on the top. Flow characteristics of the anhydrous ethanol were photographed using a high speed camera through the quartz cover. The boiling-condensation heat transfer and fluid-flow in the limited enclosed space were simulated. Effective heat transfer coefficient calculated based on the experimental data varied from 1.0-1.1 W/°C, while that of the inner wall obtained by the simulation varied within the range of 1.068-1.076 W/°C. The maximum error was 2.9%, which verified the reliability of the simulation results. By analyzing the pressure change in condensation section, it was found that the boiling-condensation heat released in the enclosed space changed periodically, because of the growth and bursting of bubbles and falling of the working medium due to gravity. Restricted by the thickness, the bubbles produced by boiling of the working medium grew in flat and irregular shapes, promoting the upward movement of the rest of the liquid working medium, and a liquid film was formed at the heated inner surface for evaporation heat transfer, which enhanced the heat transfer capacity of the heating section.

Key words: *visualization, boiling, condensation, numerical simulation, heat pipe, heat transfer*

Introduction

As electronic devices become lighter, thinner, and highly integrated, traditional micro heat pipes cannot meet the usage requirements. Ultra-thin flat heat pipes have thus become the research focus of modern heat pipe technology. The fabrication processing and phase-change heat transfer characteristics of ultra-thin flat heat pipes are complicated. Two main fabrication methods have been used to fabricate flat heat pipes: flattening modelling and welding package modelling with two flat plates [1]. The most widely used flattening technology is the phase-

* Corresponding author, e-mail: licong0719@jxust.edu.cn

change flattening process [2]. Due to the characteristics of these two fabrication methods, the phase-change process inside the flat heat pipe cannot be directly observed.

To study the mechanism of boiling-condensation phase-change heat transfer in enclosed cavities more clearly, many researchers have conducted visual experiments on heat pipes or phase-change heat transfer in confined spaces. A series of experiments on the confinement effects during boiling heat transfer were carried out by Ishibashi and Nishikawa [3] in open and narrow vertical annular spaces as early as the end of the 1960's. Two boiling regimes, *i.e.*, the isolated bubble and coalesced bubble regimes, were observed in the confined spaces. In addition these two boiling regimes, the third boiling regime was observed by Bonjour and Lallemand [4] while analyzing flow patterns during the boiling of R-113 in open and narrow vertical spaces. Fujita *et al.* [5] analyzed the boiling heat transfer in a confined space formed by two parallel rectangular plates. They found that the heat transfer coefficient increased as the gap size decreased at moderate heat fluxes. Similar results were also found by Misale *et al.* [6]. They performed a study of pool boiling by changing the orientation and the gap size. Their results showed that the influence of the heat flux on the boiling heat transfer was not monotonic.

While considerable attention has been given to independent boiling, the interference of other phase-change phenomena, such as condensation, was not examined in previous studies. However, boiling and condensation heat transfer occur simultaneously in the enclosed cavity of an ultra-thin heat pipe. A numerical analysis on thermal hydraulic performance of a flat heat pipe was presented by Lu *et al.* [7]. The results revealed that the coupled boiling and condensation processes had a non-negligible effect on the two-phase flow behavior. Zhang *et al.* [8, 9] proposed an experimental and visualization study on co-occurring boiling and condensation phase-change heat transfer in small confined spaces. Typical images and possible explanations for the phase-change heat transfer and interactions between the boiling and condensation were presented. In Zhang's work, the height of the closed and confined spaces was 26-33 mm. Xia *et al.* [10] presented systematic experiments and visualizations on the instabilities of phase-change heat transfer for water, ethanol, and acetone in a closed space, where the distance between the evaporator and condenser was 60 mm. Wu *et al.* [11] conducted a visualization study of the startup modes and operating states of a two-phase micro-thermosiphon. A confined space with a height of 15 mm was used for the quartz tube during the experiment. The dynamic wall temperatures and gas-liquid interface evolution were observed and analyzed. Previous studies of two-phase-change heat transfer mainly focused on steady-state performance, such as the thermal resistance [12], equivalent thermal conductivity [13], and temperature uniformity [14-16]. However, few studies have focused on quasi-steady processes when boiling and condensation are simultaneously occurring in the enclosed cavities of ultra-thin flat heat pipes.

To analyze the co-occurring boiling-condensation phase-change phenomena in the enclosed cavities of ultra-thin heat pipes, it is theoretically and practically important to conduct visualization studies. The purpose of this work was to investigate the heat transfer performance and observe the processes of boiling-condensation phase-change heat transfer. Simulations of the enclosed-cavity phase-change process were also conducted to obtain information that cannot be directly observed, such as the pressure fluctuations. The results of this work provide a better understanding of the complex phase-change phenomena and establish theoretical models.

Experimental procedure and data processing

Visualization experiment set-up

In this paper, the upper plate of the test section was made of quartz. A high speed CCD camera (240 FPS) was used to capture the phase-change heat transfer process of the

boiling-condensation interactions in an enclosed cavity. The thickness of the enclosed cavity was about 1 mm. Ethanol (99%) was used as the working fluid in the enclosed cavity. The visualization experiment set-up is shown in fig. 1. The set-up contained a heating module, cooling module, visual observation and shooting device module, and data acquisition system. The dimensions of the heating and cooling areas were 5 mm × 10 mm and 40 mm × 45 mm, respectively. An approximately 1 mm thick rubber sealing gasket was placed between the quartz cover and copper bottom plate. After the cylinders were clamped, the device was rotated 90° so that the test section remained vertical, that is, the heating section was on the bottom, and the cooling section was on the top. The condensation section of the test section was cooled by cooling water with a temperature of 21°C. The cooling water was driven into the cooling copper block by a water pump, and the flow was measured and adjusted by a flow meter. Three heating resistance rods were installed in the heating copper block. The heating power was adjusted by DC-stabilized power supply. The flow rate of the cooling water was adjusted to 60 Lph. The voltage of the DC power supply was adjusted to 28.3 V, and the corresponding current was 0.88 A. Three thermocouples $T_{ch1} - T_{ch3}$ were installed in the heated copper block to determine the actual heat conducted to the bottom copper plate, as shown in fig. 1. The test sections, which included the heating copper block and cooling copper block, were wrapped with insulating wool to reduce heat leakage to the environment.

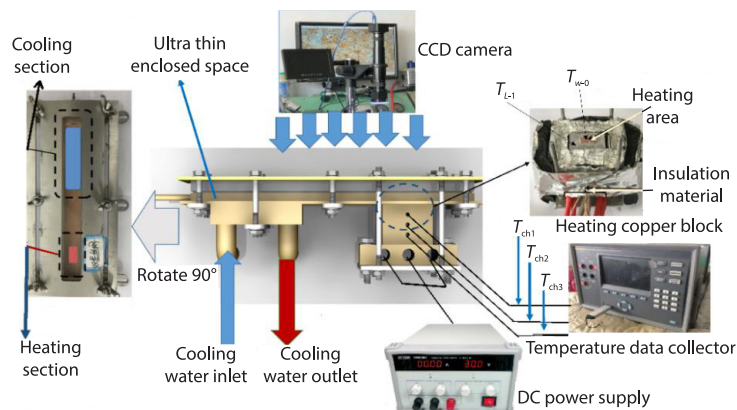


Figure 1. Schematic diagram of experimental device

Before the experiment, 800 ml of ethanol was injected into the enclosed cavity through a syringe. To ensure that the ethanol vapor produced by ethanol boiling in the heating section in the enclosed cavity effectively condensed in the cooling section, and the saturation temperature of ethanol vapor was set higher than the cooling water temperature by adjusting the pressure. To prevent the quartz from fogging and hindering the visualization, the saturation temperature of ethanol vapor was set to be lower than the ambient temperature of 24 °C. To achieve this, the pressure inside the enclosed cavity was set to 7500 Pa, the saturation temperature of ethanol was about 23 °C. Before the experiment, the enclosed cavity sealing performance was checked.

Experimental data processing

The measured data of the three thermocouples installed vertically in the heating copper block were used to calculate the actual heat flux, Q_m , that was conducted to the bottom plate of the ultra-thin enclosed cavity and the contact surface temperature, T_{w-0} , based on Fourier's Law. A layer of thermal grease was applied between the heating copper block and the bot-

tom plate. Thickness and thermal conductivity of the thermal grease were about 0.03 mm and 3 W/m°C, respectively. The temperature of the inner surface in contact with the working fluid and the actual heat flux applied to the heating area was calculated:

$$T_{w-i} = T_{w-o} - \frac{\delta_t}{\lambda_{Cu} A_H} Q_{in} \quad (1)$$

$$Q_{in} = \frac{T_{L-1} - T_{w-o}}{\frac{\delta_{si}}{\lambda_{si} A_{si-H}} + \frac{\delta_H}{\lambda_{Cu} A_{si-H}}} \quad (2)$$

Based on the calculation with eq. (2), the actual heat flux conducted into the enclosed cavity test section was in the range of 22-22.5 W. The average value of 21.75 W was selected for further analysis. A superheat-dependent effective heat transfer coefficient (EHTC) [17], h_{boil} , was extracted from the experimental data for Q_{in} and the superheat ΔT :

$$h_{boil} = \frac{Q_{in}}{A_H \Delta T} \quad (3)$$

Mathematical model description and solution strategy

The commercial software FLUENT and volume of fluids multi-phase flow method were employed to analyze the phase change and two-phase flow in the ultra-thin enclosed cavity.

Governing equations

The mass momentum and energy conservation equation are listed:

$$\frac{\partial}{\partial t} (\alpha_q \rho_q) + \nabla (\alpha_q \rho_q v_q) = S_{\alpha_q} + \sum_{p=1}^n (\dot{m}_{pq} - \dot{m}_{qp}) \quad (4)$$

$$\frac{\partial}{\partial t} (\rho \vec{v}) + \nabla (\rho \vec{v} \vec{v}) = -\nabla p + \nabla \left[\mu (\nabla \vec{v} + \nabla \vec{v}^T) \right] + \rho \vec{g} + \vec{F} \quad (5)$$

$$\frac{\partial}{\partial t} (\rho E) + \nabla [\vec{v} (\rho E + p)] = \nabla (k_{eff} \nabla T) + S_h \quad (6)$$

The influences of the surface tension are expressed through the continuum surface model by adding a source term in the momentum equation [18]:

$$S_{CSF} = 2\sigma_{lv} \frac{\alpha_l \rho_l C_v \nabla \alpha_v + \alpha_v \rho_v C_l \nabla \alpha_l}{\rho_l + \rho_v} \quad (7)$$

Phase-change model over vapor-liquid interface

A pressure-based phase-change model was used in the CFD simulation. The volumetric mass flux over the vapor-liquid interface [19] was calculated:

$$m_{lv} = \frac{6\alpha}{D_{sm}} \frac{\alpha_c}{\sqrt{2\pi}} \sqrt{\rho_v} \frac{p - p_{sat}(T)}{\sqrt{p}} \quad (8)$$

The trigger condition of the phase change in the enclosed cavity is based on the comparison of the local pressure and the saturation pressure at the corresponding local temperature,

which is different from the Lee model based on the saturation temperature. Vaporization-condensation at the interfaces occurs as long as $p_{\text{sat}}(T)$ is greater/less than p . However, the activation of nucleation boiling sites in the heating region begins at a certain super-heating condition. The super-heating condition leads to a pressure potential difference [20] Δp_i needed for growing the trapped vapor in the cavities in the heating region.

Model geometry and solution strategy

A full-scale, 3-D, transient simulation of the ultra-thin enclosed cavity model was conducted. The test section was oriented vertically. The boiling section was at the bottom, and the condensation section was at the top. The modelling geometry is shown in fig. 2. The dimensions of the enclosed cavity were 124 mm × 14 mm × 1 mm. A constant heat flux of 435000 W/m² was imposed at the bottom surface of the copper plate. A constant temperature in the cooling region was employed, and the temperature of the cooling water was set as 294 K. Side surfaces of the test section were set as heat transfer boundaries, which included natural-convection and heat radiation. The external thermal emissivity of the copper was set as 0.22. The other outer boundary surfaces were assumed to be thermally insulated. The density of ethanol vapor was calculated based on the ideal gas law.

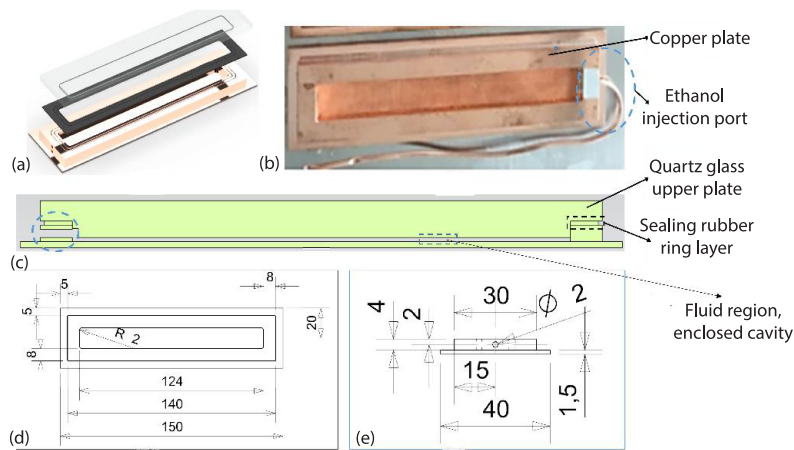


Figure 2. Geometry of the ultrathin limited enclosed space and test device

Table 1. Relative error of the inner heating surface between the simulation data and experimental data

Number of grid cells	15228	30224	61664	108133	112373	149194
Relative error [%]	1.77	1.21	1.21	0.98	0.95	0.94

The computational geometry was discretized using a hexahedral structured grid. The volume formulation was discretized by the Geo-Reconstruct scheme to track the liquid-vapor interface. A second-order upwind scheme was used to discretize the momentum and energy equations. The SIMPLE algorithm was adopted for the pressure-velocity coupling. The time step size was $1 \cdot 10^{-4}$ second. Grid refinement test was performed for the heat output at steady-state, and the total number of grid cells was 108133, according to the results as shown in tab. 1.

Results and discussion

Data analysis and simulation verification

Figure 3 shows the variation of the measured temperature of the inner wall as the temperature was about to reach a dynamic and stable variation period. The inner wall was where the heating section was in contact with the liquid working medium. The experimental and simulation data were shown in figs. 4(a) and 4(b), respectively. Fluctuations occurred both during the temperature rise process and after the temperature reached dynamic stability. The mean temperature of the inner wall in experimental data was $44.5\text{ }^{\circ}\text{C}$, while the mean temperature obtained by numerical simulation was $44.06\text{ }^{\circ}\text{C}$, with an error of about 0.98%. In the temperature rise process, bubbles formed and grew rapidly in the enclosed space, which squeezed the flow of the liquid working medium. When the bursting of the bubbles formed in the boiling process and the condensation process reached dynamic equilibrium, the flow of the working medium in the enclosed space changed periodically, and the duration of the periodic temperature fluctuations increased.

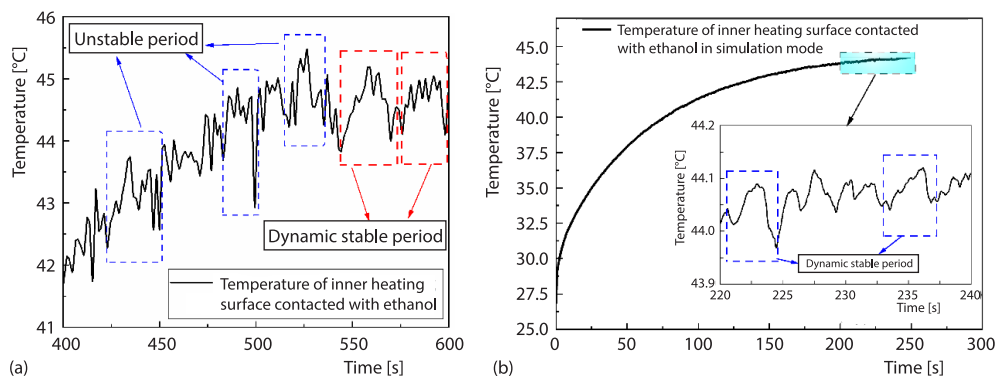


Figure 3. Temperature variation at the heated inner surface; (a) experiment data and (b) simulation data

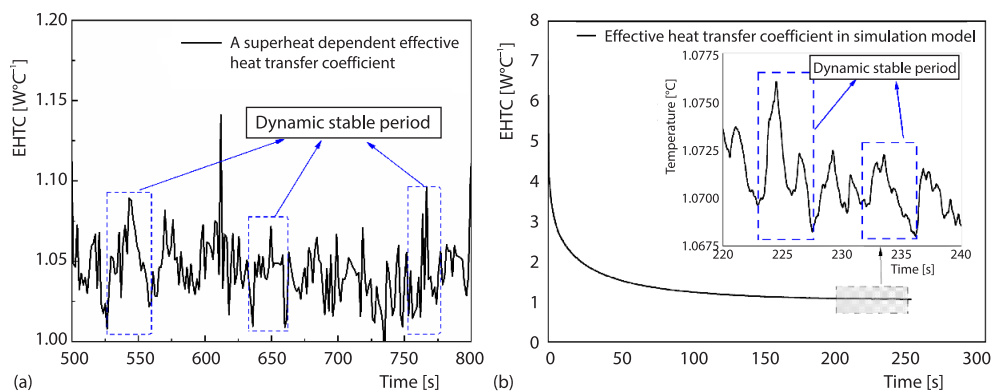


Figure 4. Variation of EHTC at the heated inner surface based on the degree of superheating; (a) experiment data and (b) simulation data

Figure 4 shows the variation of the EHTC of the boiling-condensation heat transfer process in the heating section over time in the dynamic equilibrium stage. The EHTC was related to the EHTC of the working medium on the inner wall, where the boiling re-

gion was in contact with the heating wall. As shown in fig. 4(a), the EHTC also fluctuated periodically. Such periodic fluctuations may relate to the formation and bursting of bubbles generated by boiling in the heating section within the enclosed space. Furthermore, there was a maximum boiling heat transfer coefficient in each period. Figure 4(b) shows the change of the EHTC of the working medium obtained by numerical simulation. Similar to fig. 4(a), fig. 4(b) also features periodic changes, which may be caused by the growth and bursting of bubbles in the boiling region and the reflux of the liquid working medium to the heating section under the action of gravity. The EHTC of the heated inner surface calculated based on the experimental data was in the range of 1.0-1.1 W/°C, while the EHTC obtained by numerical simulation was in the range of 1.068-1.076 W/°C, with a maximum error of 2.9% between the two. Therefore, the reliability of the results obtained by the numerical simulation model was verified.

Visualization and simulation

Figure 5 shows the structure of the 3-D flat heat pipe with an ultrathin enclosed space, the distribution of the temperature, fig. 5(a), and volume fraction, fig. (5b) of the working medium in the ultrathin limited enclosed space. The temperature contour in fig. 5(a) shows that temperature of the enclosed space was higher than the solid region where heat conduction occurred. The distribution of the liquid-phase volume fraction in the ultrathin enclosed space was shown when the boiling-condensation reached a dynamic stable stage. In the heating section, anhydrous ethanol absorbed heat and boiled to produce a large number of bubble cores. When the bubbles grew and squeezed each other in the limited space, the liquid working medium in the boiling region moved upward, driven by the bubbles, and occupied about half of the inner enclosed space.

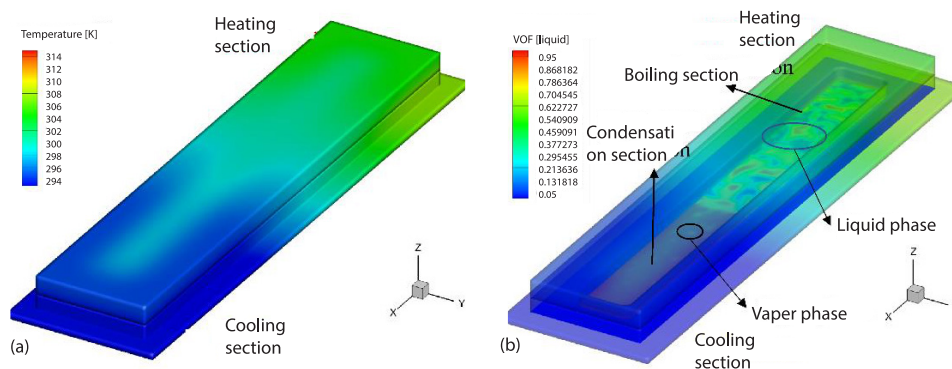


Figure 5. Distribution of the temperature (a) and liquid phase volume fraction (b) in the ultrathin limited enclosed space

As previously stated and shown in fig. 4, there was an optimal EHTC within a period, which was likely due to the periodic variations of the flow state of the working medium during the boiling process. During the heating and boiling processes, when a specific superheat degree was reached, boiling bubble cores formed at the heated inner surface, as shown in fig. 6. The growing bubbles, which were restricted by the enclosed space in the thickness direction, squeezed the surrounding liquid working medium, forming bubbles with flat and irregular shapes. As the bubbles grew to certain sizes, they drove the surrounding liquid working medium to move upward. At this time, since the bubbles occupied a significant amount of space

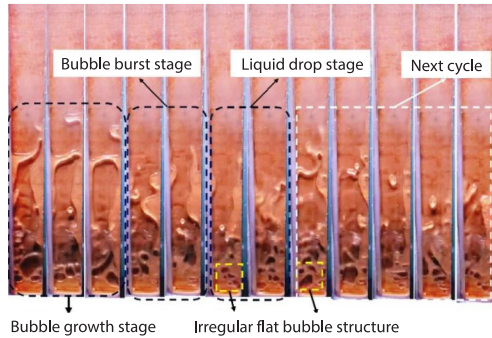


Figure 6. Photographs of anhydrous ethanol flow characteristics in the limited enclosed space

of the liquid working medium in the heating area increased. Consequently, the heat transfer capacity of the phase transition declined gradually and was turned into a convective heat transfer process with the liquid working medium, resulting in an increase in the temperature of the heated inner surface. Once the temperature at the heated inner surface reached a certain degree of superheating, new bubbles were produced, and the next cycle of heat transfer began.

Figure 7 shows the distribution of volume fraction of anhydrous ethanol during the phase transition process in the effective enclosed space obtained from the simulation. The flow characteristics of the liquid anhydrous ethanol during boiling-condensation heat transfer obtained based on simulation were similar to the photographs from the visualization experiments, fig. 6. In the heating section, the working medium absorbed heat, and bubble cores were generated. In addition, with the increase of heating area temperature, the bubbles grew rapidly, fig. 7(b). As the degree of superheating of the heated inner surface increased, the number of generated bubble cores increased, and the transition from figs. 7(b) and 7(c) was caused by the rapid growth and mutual squeezing of the bubbles. Driven by the growing bubbles, the liquid working medium continued moving forward until the bubbles burst, and the liquid working medium fell back to the boiling region under the action of gravity, repeatedly moving upward under the action of new bubbles and then falling again. Due to the growth of the bubbles, the rise and fall of the liquid working medium in the boiling region, and the heated inner surface being repeatedly covered by a bubble film and the liquid working medium, periodic fluctua-

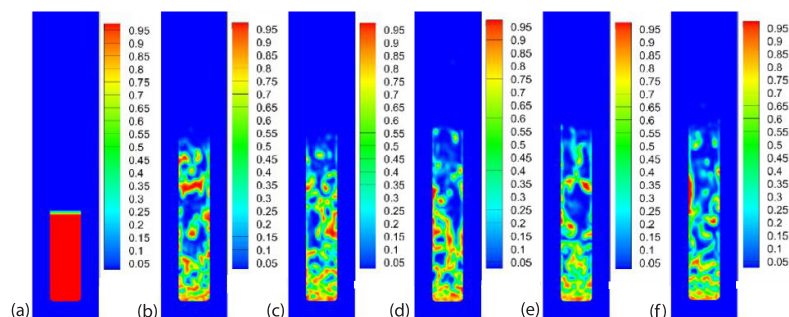


Figure 7. Distribution of volume fraction of anhydrous ethanol during phase transition process in the limited enclosed space obtained from simulation;
(a) $t = 0$ seconds, (b) $t = 32.07$ seconds, (c) $t = 33.07$ seconds,
(d) $t = 34.07$ seconds, (e) $t = 35.07$ seconds, and (f) $t = 36.07$ seconds

in the heating section, the heated inner surface was covered by the bubble film to form a liquid film evaporator, which increased the heat transfer performance and decreased the temperature at the heated inner surface. This is similar to the conclusion of Katto *et al.* [21]. Their results revealed that the increase in the thickness of the evaporating thin film between the vapor bubble and the heated wall enhanced the boiling heat transfer.

As the bubbles grew to a certain volume, they squeezed and ruptured the surrounding liquid film. Therefore, the liquid working medium fell under the action of gravity, and the volume

tions were found in the degree of superheating, EHTC, and temperature at the inner wall of the boiling section of the enclosed space.

Figure 8 shows the fluctuation of the average pressure in condensation section. The middle position of the cavity of the condensation section ($z = 2$ mm) was used as the pressure data collection surface. When the phase change heat transfer process in the confined space reaches dynamic stability, the pressure of the cavity in the condensing section exhibits periodic fluctuations, which were similar to the temperature fluctuations of the heating section. The fluctuation of pressure was caused by the growth and bursting of bubbles, reflux of liquid working medium and the condensation of ethanol vapor. The pressure in condensation section was in the range of 10103-10824 Pa, which was higher than the initial pressure value (7500 Pa). Increase of the pressure may be caused by the accumulation of ethanol vapor released by the flat and irregular bubbles.

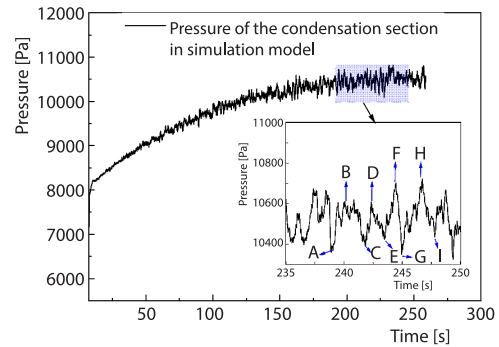


Figure 8. Variation of the pressure in the condensation section obtained from simulation

The pressure in condensation section was in the range of 10103-10824 Pa, which was higher than the initial pressure value (7500 Pa). Increase of the pressure may be caused by the accumulation of ethanol vapor released by the flat and irregular bubbles.

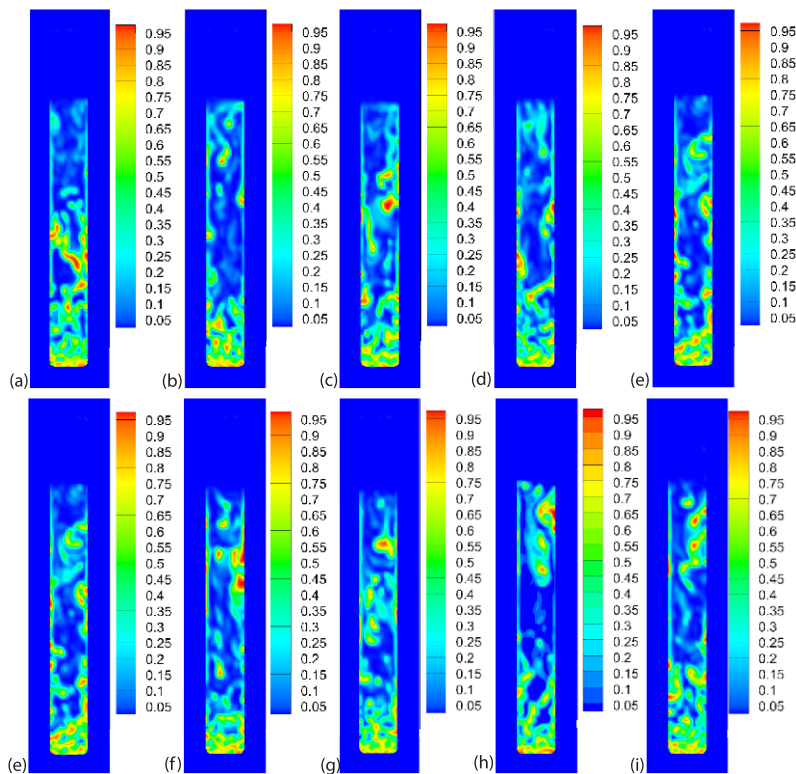


Figure 9. Distribution of volume fraction of anhydrous ethanol during phase transition process marked (a ~ i) in pressure fluctuation curve, fig. 8; (a) $t = 238.91$ seconds, (b) $t = 240.03$ seconds, (c) $t = 241.79$ seconds, (d) $t = 242.31$ seconds, (e) $t = 243.47$ seconds, (f) $t = 244.47$ seconds, (g) $t = 244.95$ seconds, (h) $t = 246.67$ seconds, and (i) $t = 247.79$ seconds

To further analyze the characteristics of periodic fluctuations of pressure, peaks and troughs in the pressure fluctuation curve were marked from A to I, respectively. The distribution of the liquid phase volume fraction corresponding to the marked characters was shown in fig. 9. The pressure peak occurred when the irregular bubbles grew to the maximum, ruptured and released amounts of ethanol vapor to the condensation section. The trough appeared when the reflux of liquid working medium occurred by the action of gravity, and the condensing of ethanol vapor. The pressure dropped until the next cycle of flat bubble growth and bursting. The characteristics of the boiling and condensation in enclosed space obtained could provide a meaningful reference for enhancing the boiling heat transfer capability of ultra-thin heat pipes.

Conclusions

This study conducted a visualization experiment and simulations to explore the flow characteristics and heat transfer mechanism of anhydrous ethanol phase-change heat transfer in an ultra-thin enclosed space. Reliability of the numerical simulation model was verified by comparing the experimental data with the simulation results. The EHTC calculated based on the experimental data varied from 1.0-1.1 W/°C, while that of the inner wall obtained by the simulation varied within the range of 1.068-1.076 W/°C, with the maximum error of 2.9%. By analyzing the pressure change in the condensation section, the growth characteristics of bubbles in the limited enclosed space and the influences on the boiling-condensation heat transfer were analyzed. Conclusions are as follows.

- Due to the growth of the bubbles and gravity, the liquid working medium in the boiling region rose and fell periodically. This flow feature caused the heated inner surface being repeatedly covered by a bubble film and the liquid working medium. Periodic fluctuations were found in the temperature at the inner wall of the boiling section of the enclosed space, and pressure in condensation section.
- Restricted by the thickness, the bubbles produced by the boiling of the working medium grew in flat and irregular shapes, promoting the upward movement of the rest of the liquid working medium, and a liquid film was formed at the heated inner surface for evaporation heat transfer, which enhanced the heat transfer capacity of the heating section.

Acknowledgment

This research was supported by the Foundation for Doctors of Jiangxi University of Science and Technology (No. 3401223407), and Jiangxi Provincial Department of Education Science and Technology Program (No. GJJ190492).

Nomenclature

A – area, [m²]

C – mean curvature, [m]

D_{sm} – mean Sauter diameter, [m]

E – internal energy, [Jm⁻³s⁻¹]

\vec{F} – force field, [N]

\vec{g} – gravity, [ms⁻²]

h_{boil} – effective heat transfer coefficient, [W°C⁻¹]

k_{eff} – effective thermal conductivity, [Wm⁻²°C⁻¹]

\dot{m} – mass transfer rate, [kgm⁻³s⁻¹]

m_{lv} – volumetric mass flux, [kgm⁻³s⁻¹]

p – pressure, [pa]

S_{aq} – mass source term, [kgm⁻³s⁻¹]

S_h – source term, [Wm⁻³]

S_{CSF} – surface tension force, [mNm⁻¹]

T – temperature, [K]

v – velocity, [ms⁻¹]

Greek symbols

α – phasic volume fraction

α_c – accommodation coefficient, 0.03

δ – thickness, [m]

λ – thermal conductivity, [Wm⁻²°C⁻¹]

ρ – density, [kgm⁻³]

σ_{lv} – surface tension, [Nm⁻¹]

Subscript

H – heating area

l – liquid

pq – phase p to phase q	sat – saturation
q – phase q	t – copper plate thickness
qp – phase q to phase p	v – vapor
si – thermal grease	w-i – boiling section inner surface
si-H – interface between thermal grease and the bottom of copper plate	w-o – boiling section outer surface

References

- [1] Yong, T., et al., Development Status and Perspective Trend of Ultra-thin Micro Heat Pipe, *Journal of Mechanical Engineering*, 53 (2017), 20, pp. 131-144
- [2] Jiang, L., et al., Phase Change Flattening Process for Axial Grooved Heat Pipe, *Journal Of Materials Processing Technology*, 212 (2012), 1, pp. 331-338
- [3] Ishibashi, E., Nishikawa, K., Saturated Boiling Heat Transfer in Narrow Spaces, *International Journal of Heat and Mass Transfer*, 12 (1969), 8, pp. 863-893
- [4] Bonjour, J., Lallemand, M., Flow Patterns during Boiling in a Narrow Space between Two Vertical Surfaces, *International Journal of Multi-phase Flow*, 24 (1998), 6, pp. 947-960
- [5] Fujita, Y., et al., Nucleate Boiling Heat Transfer and Critical Heat Flux in Narrow Space between Rectangular Surfaces, *International Journal of Heat and Mass Transfer*, 31 (1988), 2, pp. 229-239
- [6] Misale, M., et al., The HFE-7100 Pool Boiling Heat Transfer and Critical Heat Flux in Inclined Narrow Spaces, *International Journal of Refrigeration*, 32 (2009), 2, pp. 235-245
- [7] Lu, L., et al., Numerical Analysis on Thermal Hydraulic Performance of a Flat Plate Heat Pipe with Wick Column, *Heat And Mass Transfer*, 51 (2015), 8, pp. 1051-1059
- [8] Zhang, G., et al., An Experimental Study of Boiling and Condensation Co-Existing Phase Change Heat Transfer in Small Confined Space, *International Journal Of Heat And Mass Transfer*, 64 (2013), 2, pp. 1082-1090
- [9] Zhang, G., et al., A Visualization Study of the Influences of Liquid Levels on Boiling and Condensation Co-Existing Phase Change Heat Transfer Phenomenon in Small Confined Spaces, *International Journal of Heat and Mass Transfer*, 73 (2014), pp. 415-423
- [10] Xia, G., et al., Visualization Study on the Instabilities of Phase-Change Heat Transfer in a Flat Two-Phase Closed Thermosyphon, *Applied Thermal Engineering*, 116 (2017), Apr., pp. 392-405
- [11] Wu, L., et al., Visualization Study of Startup Modes and Operating States of a Flat Two-Phase Micro Thermosyphon, *Energies*, 11 (2018), 9, 2291
- [12] Deng, Z., et al., Experimental Study on Thermal Performance of an Anti-Gravity Pulsating Heat Pipe and its Application on Heat Recovery Utilization, *Applied Thermal Engineering*, 125 (2017), Oct., pp. 1368-1378
- [13] Kim, H.-J., et al., The Effect of Nanoparticle Shape on the Thermal Resistance of a Flat-Plate Heat Pipe Using Acetone-Based Al₂O₃ Nanofluids, *International Journal of Heat and Mass Transfer*, 92 (2016), Jan., pp. 572-577
- [14] Blet, N., et al., Heats Pipes for Temperature Homogenization: A Literature Review, *Applied Thermal Engineering*, 118 (2017), Mar., pp. 490-509
- [15] Do, K. H., et al., A Mathematical Model for Analyzing the Thermal Characteristics of a Flat Micro Heat Pipe with a Grooved Wick, *International Journal Of Heat And Mass Transfer*, 51 (2008), 19-20, pp. 4637-4650
- [16] Jian, Q., et al., Analysis on Thermal and Hydraulic Performance of a T-Shaped Vapor Chamber Designed for Motorcycle LED Lights, *Thermal Science*, 23 (2019), 1, pp. 137-148
- [17] Tanya, L., et al., Optimization of Hybrid Wick Structures for Extreme Spreading in High Performance Vapor Chambers, *Proceedings*, 15th IEEE Intersociety Conference on Thermal and Thermomechanical Phenomena in Electronic Systems (ITherm), 2016, pp. 30-36
- [18] Brackbill, J. U., et al., A Continuum Method for Modelling Surface Tension, *Journal of Computational Physics*, 100 (1992), 2, pp. 335-354
- [19] Wang, X., et al., Development of Pressure-Based Phase Change Model for CFD Modelling of Heat Pipes, *International Journal of Heat and Mass Transfer*, 145 (2019), 118763
- [20] Reay, D. A., et al., Heat Transfer and Fluid-Flow Theory, (Eds.. D. A. Reay et al.), in: *Heat Pipes*, 6th ed., Butterworth-Heinemann, Oxford, UK, 2014, pp. 15-64
- [21] Katto, Y., et al., Nucleate and Transition Boiling in a Narrow Space between Two Horizontal, Parallel Disk-Surfaces, *Bulletin of JSME*, 20 (1977), 143, pp. 638-643